Design of a uniform bias magnetic field for giant magnetostrictive actuators applying triple-ring magnets

2013 Smart Mater. Struct. 22 115009

(http://iopscience.iop.org/0964-1726/22/11/115009)

Smart Mater. Struct. **22** (2013) 115009 (6pp) doi:10.1088/0964-1726/22/11/115009

Design of a uniform bias magnetic field for giant magnetostrictive actuators applying triple-ring magnets

Heng Zhang, Tianli Zhang and Chengbao Jiang

School of Materials Science and Engineering, BeiHang University, Beijing 100191, People's Republic of China
Key Laboratory of Aerospace Advanced Materials and Performance, BeiHang University, Ministry of Education, People's Republic of China

E-mail: tlzhang@buaa.edu.cn and jiangcb@buaa.edu.cn

Received 27 June 2013, in final form 2 September 2013
Published 3 October 2013
Online at stacks.iop.org/SMS/22/115009

Abstract
Uniform bias magnetic field is very important for giant magnetostrictive actuators (GMA) to fully utilize the performance of giant magnetostrictive materials (GMM). However, it is difficult to keep it uniform when the length to diameter ratio (α) of the GMM is larger than 3.5, though the shapes of the applied GMM are different with α usually larger than 3.5. In this paper, a design method with triple-ring permanent magnets is established to provide an even bias magnetic field for GMM with varying α. Firstly, the magnetic circuit model is set up. According to the analysis of the field distribution along the GMM rod, the main factor causing unevenness of the bias magnetic field is confirmed to be the inner leakage flux. A design of triple-ring topology for the magnets is developed to control the inner leakage flux to reduce the unevenness. Then, finite element analysis is adopted to optimize a design which can ensure an unevenness of the bias magnetic field of less than 3% while the α of a GMM rod is up to 20. Finally, an actual GMA is fabricated with the GMM dimension of $\varnothing$10 mm $\times$ 50 mm ($\alpha = 5$), and the testing results show that the unevenness of the bias field along the GMM is 1.38%. The bias magnetic system design is practicable, simple and efficient for offering an even bias magnetic field when α lies in a wide range.

(Some figures may appear in colour only in the online journal)

1. Introduction

A giant magnetostrictive material (GMM) discovered by Clark *et al* [1], commercially named Terfenol-D, has large magnetostriction up to 2000 ppm, fast response and high resolution. GMM as a key unit has been used in many kinds of microactuating devices which are important in the fields of aerospace, optical communications, robotics and other modern industries [2–8]. Because GMM elongates with increasing absolute value of the magnetic field, a bias magnetic field is required to set the initial position at the middle of the linear part of the magnetostrictive curve and eliminate the effect of doubling frequency when giant magnetostrictive actuators (GMA) are driven by an AC signal. And the performance of the GMM can be fully utilized when the unevenness of the bias magnetic field is low. An electromagnetic solenoid is commonly used to offer a bias magnetic field which is convenient for adjusting. But the solenoid will increase the weight and volume of the devices. The heat generated by the driving current in the coil requires a cooling system which makes the device complicated and raises the cost of maintenance.

Using a permanent magnet (PM) bias field is another strategy which yields a compact device, without a cooling system or power supply [9]. In the traditional GMA, the PM used is tube-shaped, and the bias field unevenness increases drastically when the ratio of the length to diameter α of the active material is larger than 3.5 [10]. In order to offer a uniform bias field to GMM with large α ($\alpha > 3.5$), a PM bias magnetic structure was designed by Zhang *et al* [11]. In their

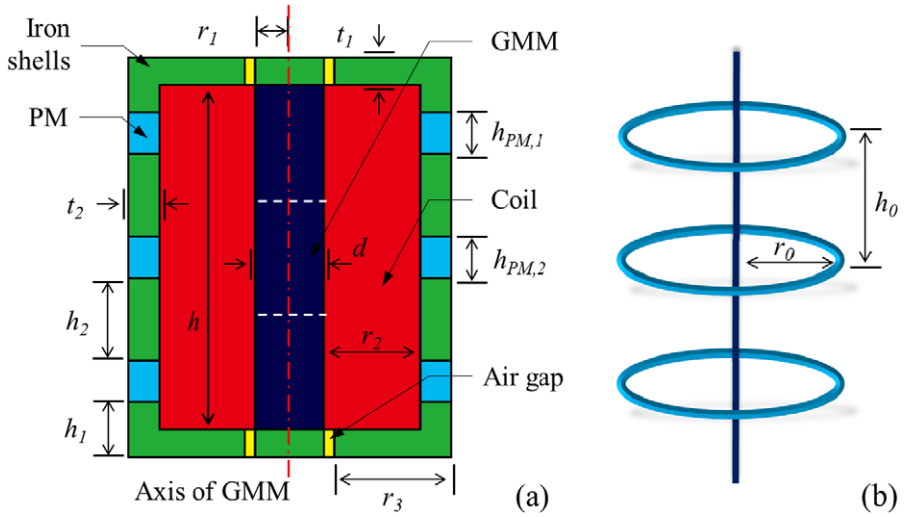

Figure 1. The simplified geometry of the magnetic circuit (a); three coaxial permanent magnet rings in open space (b).

design, compared to that of a normal permanent magnetic cylinder, the PM tube is combined with short rings which have gradually changing shape or remanence. This design can achieve an even bias field along GMM with large α; however, the processes of preparing sections of magnet rings are complicated and hard to adjust. When the sizes of GMM used in GMA are various, the bias magnetic circuits have to be designed accordingly, which is complicated and will cost a lot of time. In other designs, PM rings are used to give the bias magnetic field [12]. This kind of structure could save much permanent magnet material [13] and it is easy to provide a uniform bias field when α for the GMM is smaller than 3.5. But it is difficult to apply this structure for GMM with large α because too many parameters should be confirmed by analysis and calculation. And these parameters are changing with the shape of the GMM. It is necessary to access a general design method for this bias field system, which is simple, economical and efficient, for GMA with varied α. Nevertheless, general design methods are seldom reported.

Therefore, establishment of a general design method based on PM ring structure is valuable and it can be used for different GMM rods to provide a uniform bias magnetic field. In this paper, a compact topology for a bias magnetic circuit is designed. And a magnetic circuit model and finite element simulation are adopted to optimize the design for the magnetic bias. As a result, a typical design method with triple-ring permanent magnets is developed to provide bias magnetic field, and the configurations can be used for GMA with a wide range of ratios of length to diameter of the GMM ($\alpha \leq 20$).

2. The magnetic circuit model

In the basic structure of GMA, the magnetic circuit is composed of PM, iron shells, air gaps, coil and GMM, as shown in figure 1(a). In order to suit GMM rods with large range of α, three identical permanent rings are used to provide bias magnetic field in the structure. And the GMM rod is considered as three equal sections in order to estimate the field variations when the magnetic circuit is modeled.

The flux generated by each PM ring has three parts. The first part of the flux gets through the iron shells, air gaps and GMM rod, and the strength of this part of the flux is the same in the three sections of the GMM rod. The second part of the flux leaks into the air outside the GMA. And the third part of the flux, the inner leakage flux, gets across the coil which provides an excited magnetic field for the GMM then through the rod. This part of the flux has a great effect on the unevenness of the magnetic field along a GMM rod. Changes of the distance between the PM rings and the diameter of the PM ring will cause the distribution of this part of the flux to become different. Therefore, setting the three rings with appropriate diameter at the proper places is an available approach for improving the evenness of the bias field. The position of the rings can be confirmed by calculation.

According to analysis, the character of the inner leakage flux is similar to the character of the flux generated by three permanent magnet rings which are set coaxially in open space as shown in figure 1(b). In figure 1(b), the diameter of the PM rings is r_0; the distance between the PM rings is h_0. And $r_0 = r_2, h_0 = h_2$. The flux density ($B_{x,\mathrm{m}}$) of the third part provided by the middle magnet ring at any point along the axis of the GMM can be calculated on the basis of the Biot–Savart law [14]:

$$B_{x,\mathrm{m}} = \frac{B_{\mathrm{l,m}}}{2(r_2^2 + x^2)^{\frac{3}{2}}}. \tag{1}$$

And the flux density of the third part provided by the other two magnet rings can be obtained from similar equations. The inner leakage flux B_x produced by three PM rings at any point along the axis of the GMM is

$$B_x = \frac{B_{\mathrm{l,e,u}} r_2^2}{2[r_2^2 + (h_2 + x)^2]^{\frac{3}{2}}} + \frac{B_{\mathrm{l,m}} r_2^2}{2(r_2^2 + x^2)^{\frac{3}{2}}} + \frac{B_{\mathrm{l,e,d}} r_2^2}{2[r_2^2 + (h_2 - x)^2]^{\frac{3}{2}}} \tag{2}$$

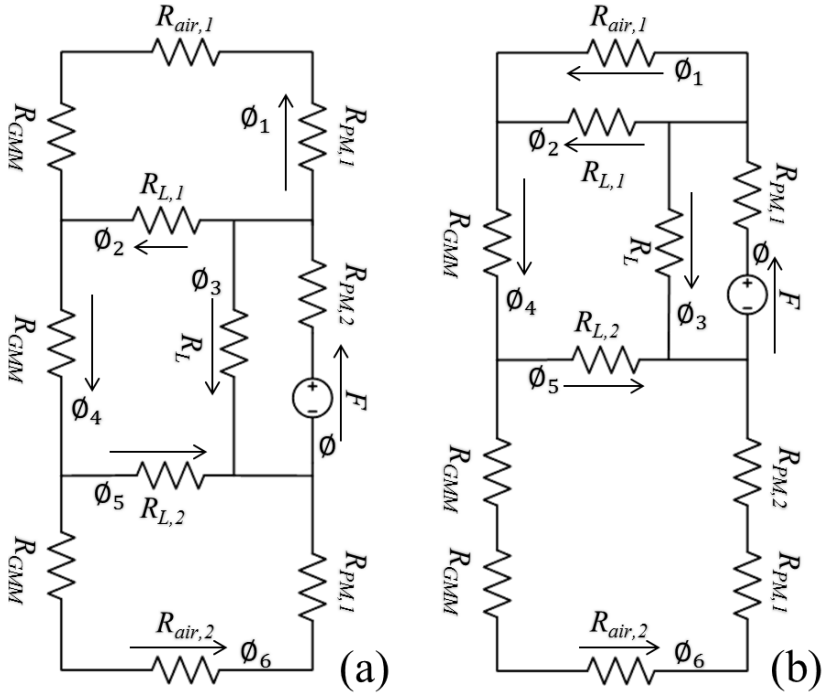

Figure 2. The magnetic circuit of the permanent magnet ring at the middle (a) and the end (b).

where $B_{\mathrm{l,e,u}}$, $B_{\mathrm{l,m}}$ and $B_{\mathrm{l,e,d}}$ are flux densities produced by each of the rings of the inner leakage flux, and r_2 is the difference between the GMM rod's radius and the PM ring's inner radius. If the PM rings are replaced by equivalent coils, and the two adjacent coils are placed as Helmholtz coils, the field along the GMM rod will be uniform [15]. Therefore, PM rings are set in terms of Helmholtz coils: the parameter r_0 equals h_0 which means that $r_2 = h_2$. And the results of the calculation from equation (2) show that the distribution of B_x along the GMM is the most uniform when $r_2 = h_2$.

Furthermore, iron shells are used to form a magnetic return path. And the iron plates at the two ends avoid the field inside the GMM diminishing sharply at the ends of the GMM rod [16]. On the other hand, the air gaps on the iron plates are used for keeping the field not too high at the ends, and they ensure that the unevenness will not get worse.

On the basis of a magnetic circuit, the magnetic circuit model of GMA is established, to analyze the field distribution along the GMM. Three permanent rings are considered respectively in the magnetic circuit model to reduce the difficulty of calculation. Figure 2(a) shows the circuit model of the permanent magnet set in the middle, and figure 2(b) is the model of the permanent magnet set at the upper end. The models of the permanent magnets at the two ends are nearly the same. In these models, the 'voltage law' and 'current law' can be applied to get the magnetic intensity H in the GMM after all reluctances of each unit are gained. The reluctance of each unit can be obtained from the definition

$$R = \int \frac{\mathrm{d}l}{\mu A} \tag{3}$$

where l is the length, μ is the permeability and A is the cross-sectional area of the unit. In the model of the permanent magnet ring at the middle, because of the symmetry of the model, the reluctances of the circuit branches R_{mu} and R_{md} are the same:

$$R_{\mathrm{mu}} = R_{\mathrm{md}} = \frac{(R_{\mathrm{gmm}} + R_{\mathrm{air},1} + R_{\mathrm{pm}}) \times R_{\mathrm{L},1}}{R_{\mathrm{gmm}} + R_{\mathrm{air},1} + R_{\mathrm{pm}} + R_{\mathrm{L},1}} \tag{4}$$

$$\phi_4 = \frac{R_{\mathrm{L}}\phi}{R_{\mathrm{mu}} + R_{\mathrm{md}} + R_{\mathrm{gmm}} + R_{\mathrm{L}}} \tag{5}$$

$$\phi_1 = \phi_6 = \frac{R_{\mathrm{L},1}\phi_4}{(R_{\mathrm{gmm}} + R_{\mathrm{air},1} + R_{\mathrm{pm}} + R_{\mathrm{L},1})} \tag{6}$$

$$H_4 = \frac{\phi_4}{\mu\pi\left(\frac{d}{2}\right)^2} \tag{7}$$

$$H_1 = H_6 = \frac{\phi_1}{\mu\pi\left(\frac{d}{2}\right)^2} \tag{8}$$

where Φ is the total magnetic flux provided by the permanent magnet ring, Φ_1 is the magnetic flux getting through the upper section of the GMM, Φ_4 is the flux getting through the middle section of the GMM and Φ_6 is the flux getting through the lower section of the GMM; H_1, H_4 and H_6 are the flux intensities of each of the sections of the GMM. In the models of the permanent magnet rings at the two ends, two other similar sets of equations can be set up to get the flux intensity along the GMM. By combining the three parts of the flux intensity together, the distribution of field along the GMM can be achieved. The unevenness of the magnetic field along the GMM is defined by the following equation:

$$\eta = \frac{\sqrt{\left[\frac{1}{N}\sum_{i=1}^{N}(H_{\mathrm{i}} - H_{\mathrm{avg}})^2\right]}}{H_{\mathrm{avg}}} \times 100\% \tag{9}$$

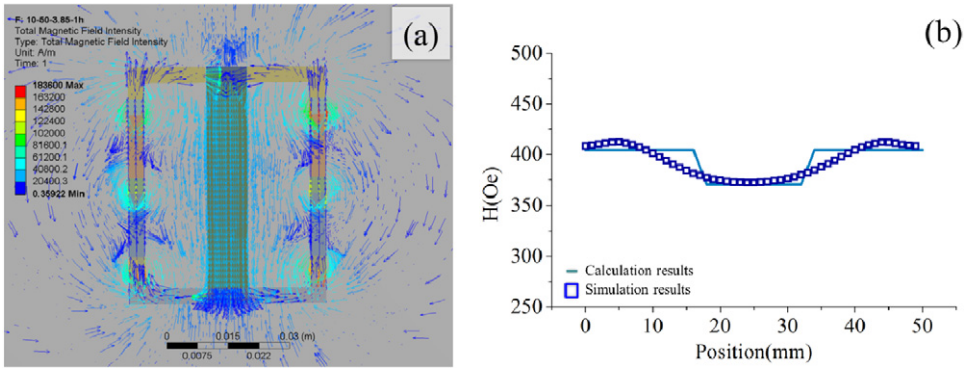

Figure 3. The result of FEA (a); magnetic field distribution in the GMM rod from calculation and FEA (b).

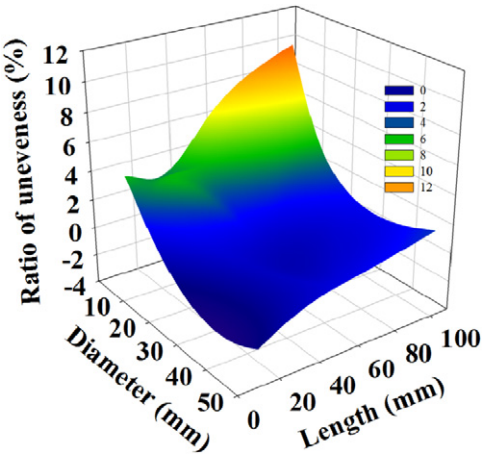

Figure 4. Unevenness of the bias magnet field in different GMM rods.

where H_i is the flux intensity along the GMM, H_{avg} is the average flux intensity along the GMM, and N is the number of data points. The GMM with 10 mm diameter and 50 mm length, as an example, is applied in the calculation. And η is 4.09%.

3. Optimization

The FEA (finite element analysis) solver, ANSYS, is applied to optimize the design method. First, the magnetic circuit with $\varnothing$10 mm $\times$ 50 mm GMM is analyzed. The triple-ring PM is set to the provide bias field. $r_2 = h_2$ is the basic rule in geometry parameter design. The simplified geometry model used in the analysis is shown in figure 1(a). In figure 3(a), the magnetic field generated by the PM rings is shown. The flux path observed in the figure is close to what we supposed in the magnetic circuit model. The magnetic field along the GMM rod is uniform (η is 3.90%). The magnetic intensities along the GMM rod obtained from calculation and FEA analysis are both plotted in figure 3(b). It can be seen that the two curves of magnetic field distributions are similar. This means that the triple-ring topology of the PM can offer a uniform magnetic field along the GMM when α is 5.

Then, whether the design method can be used with different shapes of GMM should be considered. The FEA is adopted to analyze this topology of bias magnetic field with different sizes of GMM. Several common sizes (table 1) of GMM in applications are chosen to be analyzed with the design principle mentioned above. The length of the GMM rods is from 10 to 200 mm; the diameter is from 5 to 50 mm; α is from 1 to 20. And all the bias magnetic field systems are designed on the basis of a triple-ring PM structure.

Table 1. The size of the GMM and results of analysis (η).

	Length (mm)				
Diameter (mm)	10	20	25	50	100
5	3.87%	—	3.11%	5.89%	10.01%
10	2.24%	3.56%	—	3.90%	6.42%
25	—	—	—	0.40%	1.36%
50	—	—	—	0.70%	2.03%

The results can be surface-fitted as shown in figure 4. When the diameter of the GMM is smaller, η grows faster with α increasing; when the diameter of the GMM is larger, η rises gradually. That is why the bias field, when using this design, is easier to make uniform when $\alpha < 3.5$. On the other hand, η decreases with the diameter of the GMM increasing when α is the same. And when the length is constant, the magnetic field in the GMM rod with larger diameter is more uniform.

In the FEA results, when α is smaller than 5, η stays lower than 5%. When α is 20, the unevenness η goes larger than 10%, which means that the magnetic field along the GMM is very unevenly distributed. When the ratio of length to diameter becomes larger, the magnetic field in the middle section of the GMM is much lower than it is in the other sections, as shown in figure 5. Therefore, two approaches can be applied to solve the problem. The first one is to change the remanence of the permanent magnet rings, keeping the remanence of the middle ring higher than those of the other two. The second method is to use rings with the same remanence and different thicknesses: the middle ring is thicker than the other two. In our research, the first method is chosen for convenience. After optimization, the unevenness of the magnetic field along the GMM is decreased greatly. When α is in the range 1–20, η can be kept lower than 5%. FEA results are shown in figure 5: η for the magnetic field along the $\varnothing$5 mm $\times$ 100 mm GMM goes down from 10.01% to 2.29%;

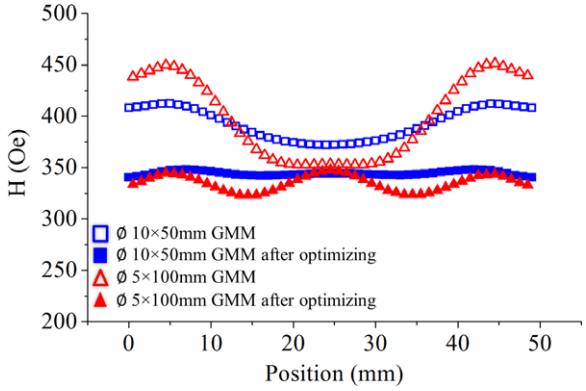

Figure 5. The results of FEA for the magnetic field along the GMM before and after optimization.

η for that along the $\varnothing$10 mm × 50 mm GMM also declines to 0.59%.

4. Validation

The GMA with $\varnothing$10 mm × 50 mm GMM ($\alpha = 5$) is processed and fabricated to validate the design. The GMA structure is shown in figure 6(a). In the bias magnetic system, three PM rings are used to provide the bias field, and the inner diameter of the PM ring equals the length of the iron shells between each of the PM rings. Figure 6(b) shows the fabricated GMA and bias magnetic system. The magnetic field along the GMM of the GMA is tested by magnetometer, and results are shown in figure 6(c): the unevenness η is 1.38%, which is similar to the results of the FEA and indicates that the bias magnetic field along the GMM is much more uniform than the traditional tube bias PM provided.

The performance of the GMA is tested. In a quasi-static test, the GMA is driven by DC power. The driven current rises from 0 to 1.5 A, then decreases to −1.5 A, and finally goes back to 0 A. During the cycle, an eddy current sensor is used to collect the data on the movements and feeds it to a PC. The captured data is analyzed by a program which can convert the signal into distance and plot it. As shown in figure 7(a), due to the appropriate bias magnetic field, the symmetrical bidirectional displacements of 20 and −21 μm are achieved.

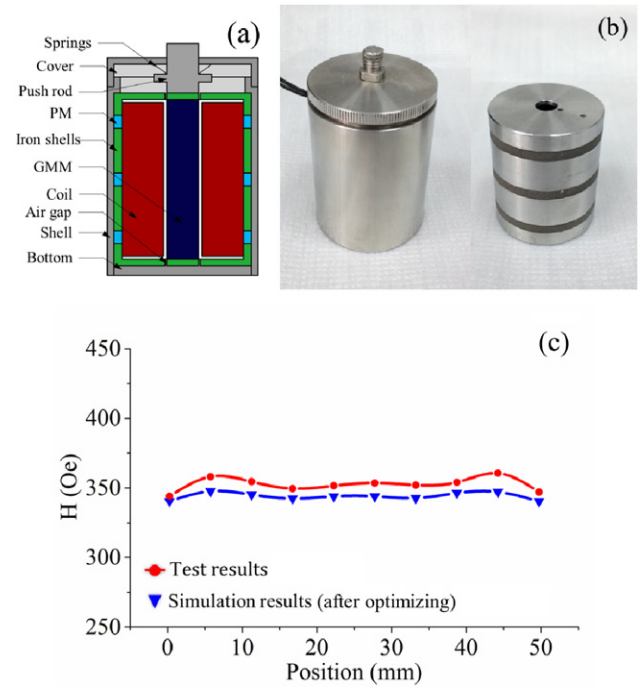

Figure 6. The structure of a GMA with three magnet rings for bias magnetic field (a); the fabricated GMA and bias magnetic system (b); results of the test and FEA for the magnetic field distribution along the $\varnothing$10 mm × 50 mm GMM (c).

In the dynamic test, the assembled GMA is set on a platform which has been fixed to the ground. The sine signal from the controller is fed to the GMA. The displacement data received from the eddy current sensor is sent to the signal acquisition unit in the controller. The test result is plotted as figure 7(b). The actual placement follows the commanded signal synchronously.

5. Conclusions

A method of design of a bias magnetic field system with a triple-ring PM is developed to adapt to various ratios of length to diameter of the GMM rod in applications. The magnetic circuit model of the GMA is established, to analyze the field

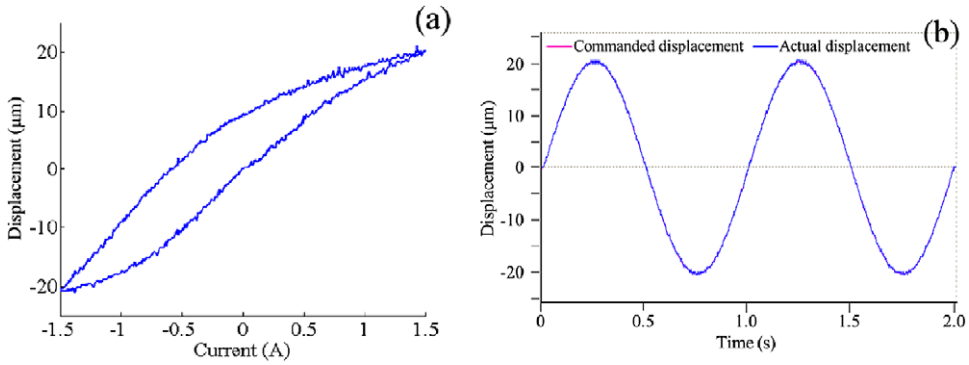

Figure 7. Quasi-static performance of the GMA driven by a 1.5 A current (a); dynamic performance of the GMA driven by a 1 Hz sine signal (b).

distribution along the GMM. Optimization by FEA ensures the unevenness of the bias magnetic field to be less than 5%, which is much lower than that for the traditional structure when $1 \leq \alpha \leq 20$. An actual GMA fabricated with the GMM dimension of $\varnothing 10$ mm $\times$ 50 mm and $\alpha = 5$ shows the unevenness of 1.38%, confirming that the method of design of the bias magnetic field system with a triple-ring PM is feasible and appropriate for achieving an even field along the GMM. The general method of design of the bias magnetic field could be used in GMA development.

Acknowledgments

The authors gratefully acknowledge the support from the National Natural Science Foundation of China (NSFC) under contracts 50925101, 51221163 and 91016006; and the National Basic Research Program of China (973 Program) under grant 2012CB619404.

References

[1] Clark A E 1980 Magnetostrictive rare earth Fe_2 compounds *Ferromagnetic Materials* vol 1, ed E P Wohlfarth (Amsterdam: North-Holland) pp 531–89

[2] Tang Z, Lv F, Xiang Z and Li M 2004 Modeling, design and control of high-speed powerful solenoid based on giant magnetostrictive material *5th World Congr. on Intelligent Control and Automation (Hangzhou, June)* vol 4, pp 3357–61

[3] Angara R, Si L and Anjanappa M 2009 A high speed magnetostrictive mirror deflector *Smart Mater. Struct.* **18** 095015

[4] Clark A E, Savage H T and Spano M L 1984 Effect of stress on the magnetostriction and magnetization of single crystal $Tb_{0.27}Dy_{0.73}Fe_2$ *IEEE Trans. Magn.* **20** 1443–5

[5] Claeyssen F, Lhermet N and Maillard T 2003 Magnetostrictive actuators compared to piezoelectric actuators *Proc. SPIE* **4763** 194–200

[6] Olabi A G and Grunwald A 2008 Design and application of magnetostrictive materials *Mater. Des.* **29** 469–83

[7] Shao L, Yang D, Chen K and Yang B 2009 Review of mechanical structure of micro-displacement actuator for optical astronomical telescope *Prog. Astron.* **27** 70–9

[8] Dhilsha R, Rajeshwari P M and Rajendran V 2005 Advanced magnetostrictive materials for sonar applications *Def. Sci. J.* **55** 13–20

[9] Grunwald A and Olabi A G 2008 Design of a magnetostrictive (MS) actuator *Sensors Actuators* A **144** 161–75

[10] Engdahl G 2002 Design procedures for optimal use of giant magnetostrictive materials in magnetostrictive actuator applications *8th Int. Conf. on New Actuators (Bremen, June)* vol 41, pp 554–7

[11] Engdahl G and Bergqvist A 1996 Loss simulations in magnetostrictive actuators *J. Appl. Phys.* **79** 4689

[12] Zhang T, Jiang C, Xu H and Mao J 2007 Permanent-magnet longitudinal fields for magnetostrictive devices *J. Appl. Phys.* **101** 034511

[13] Noh M D and Park Y W 2012 Topology selection and design optimization for magnetostrictive inertial actuators *J. Appl. Phys.* **111** 07E715

[14] Jackson J D 1999 Classical electrodynamics *Amer. J. Phys.* **67** 841

[15] Wu B 2001 *University Physics* (Beijing: Science Press) pp 360–71

[16] Zhang H, Zhang T and Jiang C 2012 Magnetostrictive actuators with large displacement and fast response *Smart Mater. Struct.* **21** 055014